

An Isoquinoline Scaffold as a Novel Class of Allosteric HIV-1 Integrase Inhibitors

Tyler A. Wilson,[†] Pratibha C. Koneru,[‡] Stephanie V. Rebensburg,[‡] Jared J. Lindenberger,[‡] Matthew J. Kobe,[§] Nicholas T. Cockroft,[†] Daniel Adu-Ampratwum,[†] Ross C. Larue,[§] Mamuka Kvaratskhelia,[‡] and James R. Fuchs^{*,†,§}

[†]Division of Medicinal Chemistry & Pharmacognosy, College of Pharmacy, The Ohio State University, Columbus, Ohio 43210, United States

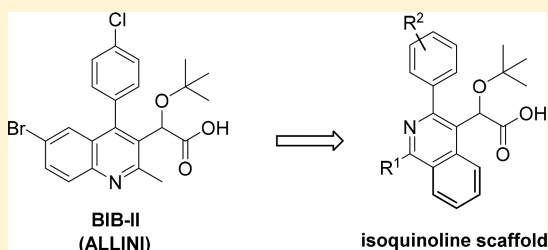
[‡]Division of Infectious Diseases, University of Colorado School of Medicine, Aurora, Colorado 80045, United States

[§]Division of Pharmaceutics & Pharmaceutical Chemistry, College of Pharmacy, The Ohio State University, Columbus, Ohio 43210, United States

Supporting Information

ABSTRACT: Allosteric HIV-1 integrase inhibitors (ALLINIs) are a new class of potential antiretroviral therapies with a unique mechanism of action and drug resistance profile. To further extend this class of inhibitors via a scaffold hopping approach, we have synthesized a series of analogues possessing an isoquinoline ring system. Lead compound **6l** binds in the v-shaped pocket at the IN dimer interface and is highly selective for promoting higher-order multimerization of inactive IN over inhibiting IN-LEDGF/p75 binding. Importantly, **6l** potently inhibited HIV-1_{NL4-3} (A128T IN), which confers marked resistance to archetypal quinoline-based ALLINIs. Thermal degradation studies indicated that at elevated temperatures the acetic acid side chain of specific isoquinoline derivatives undergo decarboxylation reactions. This reactivity has implications for the synthesis of various ALLINI analogues.

KEYWORDS: HIV-1 integrase, allosteric inhibitor, protein multimerization



Integrase (IN) is a key HIV-1 enzyme that catalyzes the integration of the viral cDNA into the host genome. In addition, IN has a second noncatalytic function, which involves IN binding to the viral RNA genome in virions to ensure correct maturation of infectious virus particles.¹ Structurally, IN functions as an oligomeric complex, with each protomer being composed of three unique domains: N-terminal domain (NTD), catalytic core domain (CCD), and C-terminal domain (CTD).² Because of the essential roles of IN in the HIV-1 life cycle, IN has been widely explored and exploited as a viable drug target for the treatment of HIV-1 infections. Initially, drug development efforts focused on disruption of the active site of IN, leading to a class of compounds referred to as IN strand transfer inhibitors (INSTIs). Three members of this class, raltegravir, elvitegravir, and dolutegravir, have ultimately become highly successful FDA approved drugs.^{3–5} However, similar to other HIV therapeutics, these compounds are susceptible to resistance mutations.^{6–8} Therefore, there is a need for the continued development of novel therapies with alternative mechanisms of action to treat HIV-1 infections.

More recently, the v-shaped pocket at the IN CCD dimer interface, which provides the principal binding site for cellular cofactor Lens Epithelium Derived Growth Factor (LEDGF/p75), has been exploited for the design of allosteric HIV-1 IN inhibitors (ALLINIs, Figure 1), which have also been

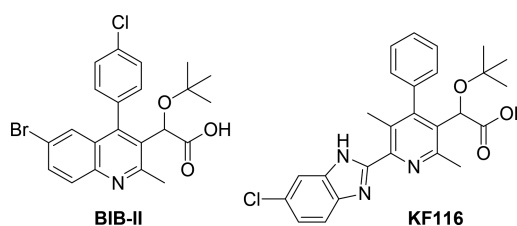


Figure 1. Chemical structures of the representative ALLINI compounds BIB-II and KF116.

alternatively referred to as LEDGINs,^{9,10} NCINIs,¹¹ and INLAIs.¹² The primary antiviral activity of these compounds is seen during virion maturation where ALLINIs induce higher-order IN multimerization and consequently impair IN-RNA interactions, which ultimately yields eccentric non-infectious virions.^{1,13–15} ALLINIs also exhibit secondary, albeit significantly reduced, activity during the early phase of HIV-1 infection, where these compounds adversely affect IN-LEDGF/p75 interactions.^{10,16}

Received: December 14, 2018

Accepted: January 30, 2019

Published: January 30, 2019

ALLINIs contain conserved structural elements attached to a substituted heteroaromatic core that allows them to mimic key interactions between LEDGF/p75 and IN dimer. The most critical ALLINI substituent is an ether-containing acetic acid side chain that engages in both hydrogen bonding and electrostatic interactions with the E170, H171, and T174 residues located in the LEDGF binding pocket of HIV-1 IN.^{17,18} An additional interaction is created by an adjacent aromatic ring that projects into a relatively narrow channel in the dimer interface capped by W132. Core ring systems such as quinoline¹⁹ and pyridine¹⁴ from which these substituents project do not provide significant binding interactions with the protein, but instead serve as rigid scaffolding units to efficiently project the substituents into the binding pocket. In addition, the decoration of these cores with methyl groups likely plays an important role in the relative orientation of the adjacent aromatic and acetic acid functional groups through conformational blocking. Despite the fact that the core ring systems may not have direct binding interactions with IN, the cores themselves have been implicated in the development of resistance mutations due to their relative size and positioning in the binding pocket. For example, a single A128T IN substitution emerges in cell culture and confers substantial resistance to archetypal quinoline-based compounds including BIB-II (Figure 1).^{6,9} Thus, these central rings impart key geometric features in addition to obvious electronic and steric properties, thereby influencing the overall potency of the ALLINIs.

In an effort to expand the scope of current ALLINIs, an alternative central ring scaffold was sought that would (1) maintain the critical C4-substituent and simultaneously facilitate substitution at the C1 and C3 positions (see numbering in Scheme 1) to capture previously unexploited contacts at the IN dimer interface, (2) exhibit full potency

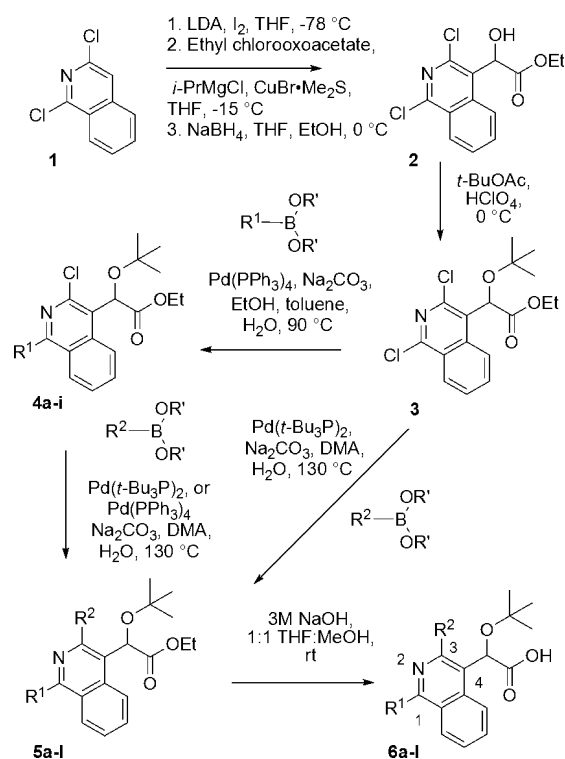
against HIV-1 containing the A128T IN substitution, which confers substantial resistance to quinoline-based ALLINIs, and (3) provide a platform for the rapid assembly of these compounds. Utilizing these criteria as a guide, an isoquinoline core was identified that could be accessed through methodology reported for the synthesis of 1,3,4-trisubstituted systems.²⁰ This isoquinoline scaffold could not only accommodate the desired substitution of the key aryl and acetic acid substituents, but the electron deficient heterocycle to which the ALLINI substituents would be attached is expected to provide a similar geometry and electronic environment to the highly potent quinoline and pyridine analogues.

The application of this approach was realized starting from the commercially available 1,3-dichloroisoquinoline (**1**). As part of a sequence to introduce the fully elaborated acetic acid side chain onto the isoquinoline, halogenation of **1** at the C4 position was affected via treatment with LDA and iodine.²⁰ The α -ketoester precursor to the acetic acid side chain was then introduced at this position via reaction of the corresponding cuprate, generated using isopropylmagnesium chloride and copper(I) bromide dimethyl sulfide complex, with ethyl chlorooxacetate following a previously reported procedure for the functionalization of quinoline and pyridine cores.²¹ In contrast, direct metalation and acylation of **1** provided only low yields (\sim 18%) of the desired product. Once installed, however, the ketoester moiety could selectively be reduced with sodium borohydride at 0 °C to provide alcohol **2**. Utilizing standard conditions for the introduction of the *t*-butyl group onto the secondary alcohol, **2** could then be converted to the desired ether **3** with the fully elaborated side chain.²¹

At this stage, **3** could be functionalized either successively or concurrently through application of appropriate coupling conditions to generate a variety of analogues. Thus, using a standard Suzuki coupling reaction, compounds **4a–i** were formed regiospecifically. More forceful coupling conditions using the more reactive bis(tri-*t*-butylphosphine)palladium(0) or a higher loading of Pd(PPh₃)₄ (40 mol % vs 20 mol %) at higher temperature could then be employed to install aryl substituents at the more sterically hindered and less reactive C3 position of the isoquinoline (**R**²) to form compounds **5a–j**. Alternatively, directly subjecting compound **3** to these “more forcing” conditions in the presence of excess boronate resulted in successive coupling at both the C1 and C3 positions in a single pot, albeit with the introduction of identical substituents at both positions. With the ethyl esters **5a–l** in hand, saponification of the ethyl group and subsequent acidification provided the desired carboxylic acids **6a–l**, representing either a six- or seven-step sequence to access the desired analogues from **1**. In nearly all cases, the carboxylic acids conveniently precipitated from solution upon acidification and could be obtained cleanly through subsequent filtration. The only exceptions were compound **6l**, a benzyl-pyrazole containing analogue, which failed to precipitate and required an additional extraction step during the course of the workup, and compound **6a**, which required a subsequent chromatographic purification step.

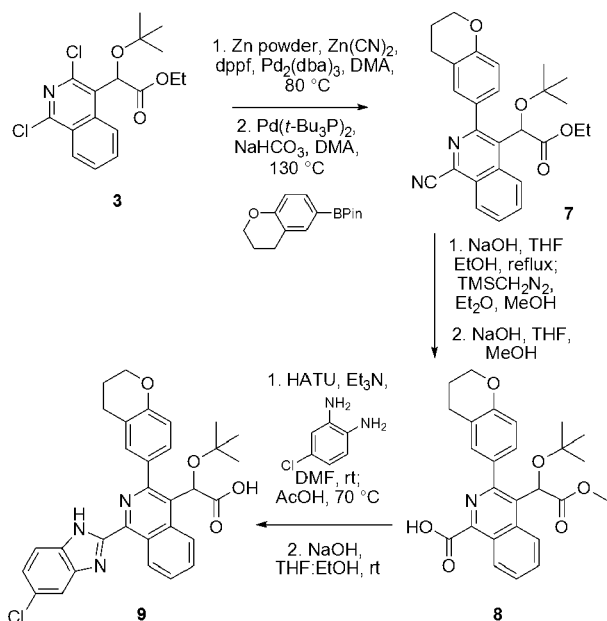
We next attempted to introduce a chlorobenzimidazole ring system at C1 to generate compound **9** based on previous observations indicating a critical role of the benzimidazole substituent for high potency of pyridine-based KF116 (Figure 1).¹⁴ While introduction of aromatic and heteroaromatic ring systems at the C1 position of the isoquinoline had been achieved through direct coupling reactions (Scheme 1), the

Scheme 1. Synthesis of Isoquinoline Analogues 6a–l



introduction of a chlorobenzimidazole ring system at this position could not be accomplished efficiently in a single coupling step. Therefore, starting from the common intermediate **3**, the nitrile group necessary for elaboration to the benzimidazole substituent was first installed via palladium-mediated coupling (Scheme 2).¹⁰ A subsequent Suzuki

Scheme 2. Synthesis of Compound 9



coupling reaction introduced the chromane system at the C3 position, providing compound **7**. In addition to the desired product, initial conditions employed for this Suzuki reaction, which included the addition of water in the presence of either sodium carbonate or sodium bicarbonate as the base, resulted in the formation of the ether byproduct **S3** (Supporting Information) produced via hydrolysis and decarboxylation of **7** along with the desired product in a 1:1.2 ratio. This decarboxylation could be eliminated under anhydrous reaction conditions while still using sodium bicarbonate as the base, producing compound **7** in a 47% yield. In order to elaborate the nitrile into the benzimidazole, a three-step sequence was carried out to affect hydrolysis of the nitrile moiety while simultaneously “maintaining” the ester functionality on the acetic acid side chain through a series of hydrolysis/esterification events to provide carboxylic acid **8**. Coupling of this acid with 4-chloro-*o*-phenylenediamine in the presence of HATU resulted in a mixture of regioisomeric amides that could be cyclized to form the benzimidazole upon heating in acetic acid. Acid **9** was then ultimately obtained through straightforward hydrolysis of the remaining ester.

The synthesized isoquinoline compounds **6a–l** and **9** were initially evaluated for their ability to inhibit IN catalytic activities in the absence of LEDGF/p75 (Table 1). The “parent” diphenyl derivatives **6a** and **6c**, both of which possess a phenyl ring at the C3 position, exhibited relatively weak inhibitory activity ($IC_{50} > 10 \mu M$). Replacement of these phenyl substituents with chromane rings in compounds **6b** and **6d** resulted in approximately 2- and 10-fold increases in potency over **6a** and **6c**, respectively. This data parallels those seen in previous SAR studies of quinoline-based ALLINIs, which also indicated improved potencies resulting from

Table 1. Chemical Structures and Inhibitory Activities (IC_{50} , μM) of Analogues Tested in LEDGF/p75 Independent Integration Assays^a

	R ¹	R ²	IC ₅₀
6a	Phenyl	Phenyl	10.1±0.89
6b	Phenyl	Chromane	4.65±1.3
6c	3-Methoxyphenyl	Phenyl	13.8±2.5
6d	3-Methoxyphenyl	Chromane	1.14±0.22
6e	4-Fluorophenyl	Chromane	12.9±3.0
6f	4-Carboxyphenyl	Chromane	12.3±2.9
6g	4-(Trifluoromethyl)phenyl	Chromane	7.64±1.5
6h	4-Methoxyphenyl	Chromane	1.00±0.15
6i	4-Phenylphenyl	Chromane	0.83±0.2
6j	4-(2-Chromanyl)phenyl	Chromane	1.22±0.3
6k	2-Furanyl	Chromane	3.55±0.19
6l	1-Benzyl-4-methyl-1H-pyrazol-5-yl	Chromane	0.48±0.01
9	4-Chlorophenyl	Chromane	0.81±0.2

^aThe standard errors from two independent experiments are indicated.

introduction of the larger chromane substituent at the C3 position.^{12,22}

The remaining analogues, **6e–l** and **9**, all possess the chromane substituent at the C3 position but vary with regard to the substitution at the C1 position. This structural consistency has facilitated direct comparison of the R¹ substituents. With this in mind, the R¹ phenyl substituents containing electron-deficient groups (**6e**, **6f**, and **6g**) demonstrated considerably less potency than the rings with electron-donating substituents (**6h** and **6j**). Moreover, regioisomeric compounds **6d** and **6h** suggest that the variation of the substituents on the phenyl ring from the meta- to para-position did not substantially affect the inhibitory activities of these compounds. The heterocycle-containing systems (**6k**, **6l**, and **9**) all showed reasonable potency as well. Among these heterocycles, the larger substituents showed greater potency. The most potent of these, the benzyl pyrazole analogue **6l**,

Table 2. Inhibitory Activities of **6l** and BIB-II in Vitro^a

inhibitor	IN multimerization, EC ₅₀ (μM)	IN-LEDGF/p75 binding, IC ₅₀ (μM)	LEDGF/p75 independent IN activity, IC ₅₀ (μM)	LEDGF/p75 dependent IN activity, IC ₅₀ (μM)	IN-RNA binding, IC ₅₀ (μM)
6l	<1.79 ± 0.19	36.7 ± 6.2	0.48 ± 0.06	23.4 ± 0.78	0.21 ± 0.03
BIB-II	0.146 ± 0.014	0.15 ± 0.01	0.12 ± 0.04	0.15 ± 0.01	0.136 ± 0.02

^aStandard errors from two independent experiments are shown.

displayed a potency of 0.48 μM. Compound **9**, which possesses the benzimidazole substituent, was approximately 2-fold less potent (IC₅₀ of 0.81 μM) than **6l**.

Our subsequent efforts have focused on elucidating the mode of action of **6l**, the most potent compound in the isoquinoline series (Table 2). For comparison, archetypal quinoline-based BIB-II was examined in parallel experiments. As expected, BIB-II¹⁹ exhibited a dual mode of action by inducing higher-order IN multimerization and inhibiting IN-LEDGF/p75 binding with comparable potency in vitro (Table 2). In contrast from BIB-II, **6l** displayed marked preference for promoting higher-order IN multimerization (EC₅₀ of <1.79 μM) compared with its ability to inhibit IN-LEDGF/p75 binding (IC₅₀ of ~37 μM). ALLINI-induced higher-order IN multimerization can in turn impair IN catalytic activities and IN-RNA interactions.^{1,19} Accordingly, BIB-II exhibited comparable EC₅₀/IC₅₀ values in all assays indicated in Table 2, whereas **6l** displayed selectivity for those assays related to higher-order IN multimerization. We noted that increasing concentrations of **6l** resulted in quenching of the donor (Europium-cryptate)-IN signal, which in turn adversely affected the measured HTRF signal increases due to inhibitor induced higher-order multimerization of IN. Therefore, **6l** could be promoting higher-order IN multimerization with even higher potency than the EC₅₀ value of 1.79 μM determined by the HTRF assay. Consistent with this notion, **6l** displayed improved IC₅₀ values of ~0.21 and ~0.48 μM for inhibiting IN-RNA binding and LEDGF/p75 independent IN catalytic activities, respectively. Compound **6l** was significantly less potent (IC₅₀ of ~23 μM) when IN activities were monitored in the presence of LEDGF/p75. The differential potencies seen in LEDGF/p75 independent vs dependent assays provide another line of evidence for marked specificity of **6l** for inducing higher-order IN multimerization over interfering with IN-LEDGF/p75 binding.

Cell culture assays compared antiviral activities of **6l** with respect to WT vs BIB-II resistant viruses. Compound **6l** inhibited WT HIV-1NL4-3 with EC₅₀ of ~1.1 μM and exhibited slightly higher potency (EC₅₀ of ~0.73 μM) with respect to HIV-1NL4-3 (A128T IN), which confers substantial resistance to BIB-II (Table 3).

Table 3. Antiviral Activities of **6l** (EC₅₀ values in μM)^a

inhibitor	HIV-1 _{NL4-3}	HIV-1 _{NL4-3} (A128T IN)
6l	1.10 ± 0.07	0.73 ± 0.07
BIB-II	0.63 ± 0.30 ¹⁹	12.2 ± 6.4 ¹⁹

^aStandard errors from two independent experiments are shown.

To elucidate the structural basis for interactions of these isoquinoline compounds with IN, we have solved the crystal structures of **6l** and its less potent predecessor **6b** bound to the CCD dimer (Figure 2). The comparative analysis of these two compounds was carried out to better understand the SAR for this series. Indeed, our structural studies allowed us to

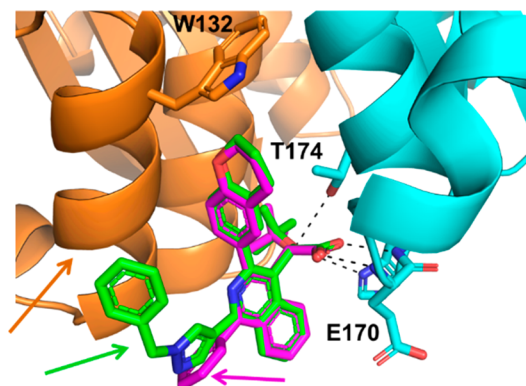


Figure 2. Crystal structures of **6b** (magenta) and **6l** (green) bound to the CCD dimer (subunits 1 and 2 are colored orange and cyan, respectively).

elucidate both similarities and differences between these two isoquinoline compounds. The carboxylic acid moiety of both compounds forms a bidentate interaction with the backbone amides of H171 and E170 of subunit 2. Additional hydrogen bonding interactions occur between H171 and T174 of subunit 2 and the ether oxygen of both compounds. The chromane rings and *t*-butoxy moieties of both compounds are situated in the hydrophobic pocket that is generated at the interface between subunits 1 and 2 and are formed by several hydrophobic residues and capped by W132.

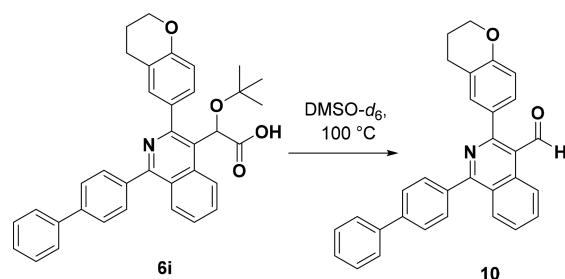
Differences between **6b** and **6l** are observed at R¹. The benzene substituent of **6b** is directed out of the dimer interface into space and has minimal interactions with CCD dimer. In contrast, the R¹ substituent of **6l** forms hydrophobic interactions with the surface of α -helix (124–133) of subunit 1, which could help to explain the substantially enhanced inhibitory activity of **6l** over **6b**.

To better understand the structural basis for differential effects of the A128T substitution on **6l** and BIB-II, we subsequently superimposed the crystal structures of these compounds (Figure S1, Supporting Information). The rigid quinoline core of BIB-II extends toward A128 and is therefore affected by the bulkier and more polar A128T substitution.¹⁹ In contrast, the isoquinoline core is substantially distanced and projects away from A128. Interestingly, the benzyl moiety on the R¹ substituent of **6l** is positioned relatively close to A128. However, the highly flexible nature of this R¹ substituent presumably allows **6l** to effectively negate the effects of the A128T substitution.

In addition to these SAR studies, the stability of the acetic acid side chains of this class of compounds was also examined. This investigation was based upon both the unexpected decarboxylation of compound **7** mentioned above and the fact that new peaks, albeit minor, were observed in the ¹H NMR spectra of several of the final carboxylic acid-containing compounds upon storage, indicating some type of decomposition. Most notably, these ¹H NMR spectra showed what appeared to be an upfield shift of the methine proton on the

acetic acid side chain. This data suggested that these compounds may be prone to decarboxylation of the acetic acid side chain. To test this hypothesis, a variation of forced degradation²³ was employed to investigate the stability of selected compounds. In this case, samples were heated in DMSO-*d*₆ in an NMR tube to expedite this degradative process and allow rapid assessment of the conversion and compound identity. Compounds **6d** and **6e**, possessing electron-deficient and electron-rich groups at the C1 position, respectively, as well as compound **6i** were initially heated at 60 °C for 17 h. The ¹H NMR spectra of each of these compounds at this time point indicated very little to no degradation (Supporting Information). After this initial period, compound **6i** was further heated by increasing the temperature to 100 °C and monitored at various time points over a period of 17 days. Interestingly, a sharp singlet at 10.12 ppm in the ¹H NMR spectrum increased in intensity over time relative to the starting material. A carbon signal at 193.6 ppm in the ¹³C NMR spectra was also observed, indicating the presence of an aldehyde peak. In the HSQC NMR spectrum, a strong correlation of the carbon signal at 193.6 ppm with the proton at 10.12 ppm also supported this assignment. Upon further examination of the ¹H NMR spectrum, a shift in the *t*-butyl ether protons from 0.90 to 1.11 ppm could also be observed, correlating with loss of the ether group, likely as *t*-butanol, during the course of the reaction. The use of high-resolution mass spectrometry in conjunction with the other spectroscopic data further supported the assignment of this compound as aldehyde **10** seen in Scheme 3.

Scheme 3. Degradation of **6i** under Thermal Conditions



The ¹H NMR spectra for compounds **6d** and **6e**, which were stored in DMSO-*d*₆ for 17 days at room temperature after the initial heating at 60 °C, revealed a similar aldehyde peak observed around ~10.1 ppm. During subsequent heating of both of these compounds to 100 °C for 3 days, the presumed aldehyde peak grew rapidly in intensity, suggesting that this degradation occurs slowly at room temperature but much faster at elevated temperatures. Surprisingly, reinvestigation of the *T*₀ (time-zero, prior to heating) ¹H NMR spectra for compound **6e** revealed the presence of a small amount of the sharp singlet at ~10.1 ppm, among other minor impurities, suggesting that the analogues with electron-withdrawing groups may be more prone to degradation upon compound storage, even at lower temperatures. To our knowledge, this is the first time that this phenomenon has been observed for a *t*-butyl ether-containing acetic acid side chain in an ALLINI compound.

The mechanism by which this decomposition happens is as of yet unknown, but it is worth noting that other groups have reported the decarboxylation of α -hydroxy carboxylic acids through chemical and enzymatic methods.^{24–28} Although 100

°C is acknowledged to not be a biologically relevant temperature, this type of degradation warrants further investigation because it could have potential implications for chemical stability of other ALLINIs as the *t*-butoxy acetic acid side chain is an important pharmacophore for all potent ALLINIs.

In conclusion, a series of isoquinoline ALLINI analogues were synthesized. Their SAR studies have revealed that sterically bulkier R¹ and R² substituents resulted in enhanced inhibitory activities of these compounds. Compound **6l**, the most active compound, exhibited markedly higher potency for inducing higher-order IN multimerization than inhibiting IN-LEDGF/p75 binding. Significantly, **6l** was highly potent against the HIV-1 variant containing the A128T IN substitution, which confers marked resistance to a number of isoquinoline-based inhibitors. The relative stability of selected isoquinoline compounds was also investigated, revealing lability in the acetic acid side chain. These observations will inform ongoing efforts in the field to synthesize various ALLINI derivatives.

■ ASSOCIATED CONTENT

Supporting Information

The Supporting Information is available free of charge on the ACS Publications website at DOI: 10.1021/acsmchemlett.8b00633.

Experimental procedures and characterization data for all compounds, thermal stability studies of compounds **6d**, **6e**, and **6i**, conditions for biological assays, and crystal structure information (PDF)

Accession Codes

PDB numbers for compounds **6b**, 6EB1, and **6l**, 6EB2.

■ AUTHOR INFORMATION

Corresponding Author

*Phone: 614-247-7377. E-mail: fuchs.42@osu.edu.

ORCID

James R. Fuchs: 0000-0002-8743-6389

Author Contributions

J.R.F., M.K., and R.C.L. conceived and designed experiments. T.A.W., P.C.K., S.V.R., J.J.L., M.J.K., N.T.C., and D.A.A. performed the experiments and analyzed the results. T.A.W., J.R.F., P.C.K., and M.K. wrote the manuscript with contributions from all other authors.

Funding

This work was supported by National Institutes of Health grants U54 GM103368 (to M.K. and J.R.F.), R21 AI138775 (to J.R.F. and R.C.L.), R01 AI062520 (to M.K.), KL2 TR001068 (to R.C.L.), and a fellowship from ST32 AT007533 (to T.A.W.).

Notes

The authors declare no competing financial interest.

■ ACKNOWLEDGMENTS

We would like to thank Dr. C. McElroy, Dr. C. Yuan, and the OSU CCIC for assistance with acquisition of NMR data.

■ ABBREVIATIONS

IN, integrase; ALLINIs, allosteric HIV-1 integrase inhibitors; LEDGF/p75, Lens Epithelium Derived Growth Factor; LEDGINS, LEDGF integrase inhibitors; NCINIs, noncatalytic

site integrase inhibitors; INLAIs, integrase-LEDGF allosteric inhibitors; HTRF, homogeneous time-resolved fluorescence

REFERENCES

- (1) Kessl, J. J.; Kutluay, S. B.; Townsend, D.; Rebusburg, S.; Slaughter, A.; Larue, R. C.; Shkriabai, N.; Bakouche, N.; Fuchs, J. R.; Bieniasz, P. D.; Kvaratskhelia, M. HIV-1 Integrase Binds the Viral RNA Genome and Is Essential during Virion Morphogenesis. *Cell* **2016**, *166*, 1257–1268.
- (2) Passos, D. O.; Li, M.; Yang, R.; Rebusburg, S. V.; Ghirlando, R.; Jeon, Y.; Shkriabai, N.; Kvaratskhelia, M.; Craigie, R.; Lyumkis, D. Cryo-EM Structures and Atomic Model of the HIV-1 Strand Transfer Complex Intasome. *Science* **2017**, *355*, 89–92.
- (3) McColl, D. J.; Chen, X. Strand Transfer Inhibitors of HIV-1 Integrase: Bringing IN a New Era of Antiretroviral Therapy. *Antiviral Res.* **2010**, *85*, 101–118.
- (4) Summa, V.; Petrocchi, A.; Bonelli, F.; Crescenzi, B.; Donghi, M.; Ferrara, M.; Fiore, F.; Gardelli, C.; Gonzalez Paz, O.; Hazuda, D. J.; Jones, P.; Kinzel, O.; Laufer, R.; Monteagudo, E.; Muraglia, E.; Nizi, E.; Orvieto, F.; Pace, P.; Pescatore, G.; Scarpelli, R.; Stillmock, K.; Witmer, M. V.; Rowley, M. Discovery of Raltegravir, a Potent, Selective Orally Bioavailable HIV-Integrase Inhibitor for the Treatment of HIV-AIDS Infection. *J. Med. Chem.* **2008**, *51*, 5843–5855.
- (5) Raffi, F.; Wainberg, M. A. Multiple Choices for HIV Therapy with Integrase Strand Transfer Inhibitors. *Retrovirology* **2012**, *9*, 110–113.
- (6) You, J.; Wang, H.; Huang, X.; Qin, Z.; Deng, Z.; Luo, J.; Wang, B.; Li, M. Therapy-Emergent Drug Resistance to Integrase Strand Transfer Inhibitors in HIV-1 Patients: A Subgroup Meta-Analysis of Clinical Trials. *PLoS One* **2016**, *11*, e0160087.
- (7) Wijting, I. E. A.; Lungu, C.; Rijnders, B. J. A.; van der Ende, M. E.; Pham, H. T.; Mesplede, T.; Pas, S. D.; Voermans, J. J. C.; Schuurman, R.; van de Vijver, D. A. M. C.; Boers, P. H. M.; Gruters, R. A.; Boucher, C. A. B.; van Kampen, J. J. A. HIV-1 Resistance Dynamics in Patients With Virologic Failure to Dolutegravir Maintenance Monotherapy. *J. Infect. Dis.* **2018**, *218*, 688–697.
- (8) Wijting, I.; Rokx, C.; Boucher, C.; van Kampen, J.; Pas, S.; de Vries-Sluijs, T.; Schurink, C.; Bax, H.; Derksen, M.; Andrinopoulou, E.-R.; van der Ende, M.; van Gorp, E.; Nouwen, J.; Verbon, A.; Bierman, W.; Rijnders, B. Dolutegravir as Maintenance Monotherapy for HIV (DOMONO): A Phase 2, Randomised Non-Inferiority Trial. *Lancet HIV* **2017**, *4*, e547–e554.
- (9) Desimmie, B. A.; Demeulemeester, J.; Christ, F.; Debyser, Z. Rational Design of LEDGINs as First Allosteric Integrase Inhibitors for the Treatment of HIV Infection. *Drug Discovery Today: Technol.* **2013**, *10*, e517–e522.
- (10) Christ, F.; Voet, A.; Marchand, A.; Nicolet, S.; Desimmie, B. A.; Marchand, D.; Bardiot, D.; Van der Veken, N. J.; Van Remoortel, B.; Strelkov, S. V.; De Maeyer, M.; Chaltin, P.; Debyser, Z. Rational Design of Small-Molecule Inhibitors of the LEDGF/P75-Integrase Interaction and HIV Replication. *Nat. Chem. Biol.* **2010**, *6*, 442–448.
- (11) Balakrishnan, M.; Yant, S. R.; Tsai, L.; O'Sullivan, C.; Bam, R. A.; Tsai, A.; Niedziela-Majka, A.; Stray, K. M.; Sakowicz, R.; Cihlar, T. Non-Catalytic Site HIV-1 Integrase Inhibitors Disrupt Core Maturation and Induce a Reverse Transcription Block in Target Cells. *PLoS One* **2013**, *8*, e74163.
- (12) Le Rouzic, E.; Bonnard, D.; Chasset, S.; Bruneau, J.-M.; Chevreuil, F.; Le Strat, F.; Nguyen, J.; Beauvoir, R.; Amadori, C.; Brias, J.; Vomscheid, S.; Eiler, S.; Lévy, N.; Delelis, O.; Deprez, E.; Saïb, A.; Zamborlini, A.; Emiliani, S.; Ruff, M.; Ledoussal, B.; Moreau, F.; Benarous, R. Dual Inhibition of HIV-1 Replication by Integrase-LEDGF Allosteric Inhibitors Is Predominant at the Post-Integration Stage. *Retrovirology* **2013**, *10*, 144–163.
- (13) Jurado, K. A.; Wang, H.; Slaughter, A.; Feng, L.; Kessl, J. J.; Koh, Y.; Wang, W.; Ballandras-Colas, A.; Patel, P. A.; Fuchs, J. R.; Kvaratskhelia, M.; Engelman, A. Allosteric Integrase Inhibitor Potency Is Determined through the Inhibition of HIV-1 Particle Maturation. *Proc. Natl. Acad. Sci. U. S. A.* **2013**, *110*, 8690–8695.
- (14) Sharma, A.; Slaughter, A.; Jena, N.; Feng, L.; Kessl, J. J.; Fadel, H. J.; Malani, N.; Male, F.; Wu, L.; Poeschla, E.; Bushman, F. D.; Fuchs, J. R.; Kvaratskhelia, M. A New Class of Multimerization Selective Inhibitors of HIV-1 Integrase. *PLoS Pathog.* **2014**, *10*, e1004171.
- (15) Jentsch, N. G.; Hart, A. P.; Hume, J. D.; Sun, J.; McNeely, K. A.; Lama, C.; Pigza, J. A.; Donahue, M. G.; Kessl, J. J. Synthesis and Evaluation of Aryl Quinolines as HIV-1 Integrase Multimerization Inhibitors. *ACS Med. Chem. Lett.* **2018**, *9*, 1007–1012.
- (16) Kessl, J. J.; Jena, N.; Koh, Y.; Taskent-Sezgin, H.; Slaughter, A.; Feng, L.; de Silva, S.; Wu, L.; Le Grice, S. F. J.; Engelman, A.; Fuchs, J. R.; Kvaratskhelia, M. Multimode, Cooperative Mechanism of Action of Allosteric HIV-1 Integrase Inhibitors. *J. Biol. Chem.* **2012**, *287*, 16801–16811.
- (17) Jurado, K. A.; Engelman, A. Multimodal Mechanism of Action of Allosteric HIV-1 Integrase Inhibitors. *Expert Rev. Mol. Med.* **2013**, *15*, e14.
- (18) Slaughter, A.; Jurado, K. A.; Deng, N.; Feng, L.; Kessl, J. J.; Shkriabai, N.; Larue, R. C.; Fadel, H. J.; Patel, P. A.; Jena, N.; Fuchs, J. R.; Poeschla, E.; Levy, R. M.; Engelman, A.; Kvaratskhelia, M. The Mechanism of H171T Resistance Reveals the Importance of N δ -Protonated His171 for the Binding of Allosteric Inhibitor BI-D to HIV-1 Integrase. *Retrovirology* **2014**, *11*, 100.
- (19) Feng, L.; Sharma, A.; Slaughter, A.; Jena, N.; Koh, Y.; Shkriabai, N.; Larue, R. C.; Patel, P. A.; Mitsuya, H.; Kessl, J. J.; Engelman, A.; Fuchs, J. R.; Kvaratskhelia, M. The A128T Resistance Mutation Reveals Aberrant Protein Multimerization as the Primary Mechanism of Action of Allosteric HIV-1 Integrase Inhibitors. *J. Biol. Chem.* **2013**, *288*, 15813–15820.
- (20) Yang, H. A. Facile Synthesis of 1,3,4-Trisubstituted Isoquinolines. *Tetrahedron Lett.* **2009**, *50*, 3081–3083.
- (21) Fandrick, K. R.; Li, W.; Zhang, Y.; Tang, W.; Gao, J.; Rodriguez, S.; Patel, N. D.; Reeves, D. C.; Wu, J.-P.; Sanyal, S.; Gonnella, N.; Qu, B.; Haddad, N.; Lorenz, J. C.; Sidhu, K.; Wang, J.; Ma, S.; Grinberg, N.; Lee, H.; Tsantrizos, Y.; Poupart, M.-A.; Busacca, C. A.; Yee, N. K.; Lu, B. Z.; Senanayake, C. H. Concise and Practical Asymmetric Synthesis of a Challenging Atropisomeric HIV Integrase Inhibitor. *Angew. Chem., Int. Ed.* **2015**, *54*, 7144–7148.
- (22) Patel, P. A.; Kvaratskhelia, N.; Mansour, Y.; Antwi, J.; Feng, L.; Koneru, P.; Kobe, M. J.; Jena, N.; Shi, G.; Mohamed, M. S.; Li, C.; Kessl, J. J.; Fuchs, J. R. Indole-Based Allosteric Inhibitors of HIV-1 Integrase. *Bioorg. Med. Chem. Lett.* **2016**, *26*, 4748–4752.
- (23) Blessy, M.; Patel, R. D.; Prajapati, P. N.; Agrawal, Y. K. Development of Forced Degradation and Stability Indicating Studies of Drugs-A Review. *J. Pharm. Anal.* **2014**, *4*, 159–165.
- (24) Beebe, T. R.; Adkins, R. L.; Belcher, A. I.; Choy, T.; Fuller, A. E.; Morgan, V. L.; Sencherey, B. B.; Russell, L. J.; Yates, S. W. *J. Org. Chem.* **1982**, *47*, 3006–3008.
- (25) Cassani, C.; Bergonzini, G.; Wallentin, C.-J. Photocatalytic Decarboxylative Reduction of Carboxylic Acids and Its Application in Asymmetric Synthesis. *Org. Lett.* **2014**, *16*, 4228–4231.
- (26) Pink, J. M.; Stewart, R. Mechanism of Oxidative Decarboxylation of α -Hydroxy Acids by Bromine Water. Part I. Oxidation in Neutral and Alkaline Medium. *Can. J. Chem.* **1971**, *49*, 649–653.
- (27) Mead, J. F.; Levis, G. M. Enzymatic Decarboxylation of the α -Hydroxy Acids by Brain Microsomes. *Biochem. Biophys. Res. Commun.* **1963**, *11*, 319–324.
- (28) Paine, T. K.; Paria, S.; Que, L. Oxidative Decarboxylation of α -Hydroxy Acids by a Functional Model of the Nonheme Iron Oxygenase, CloR. *Chem. Commun.* **2010**, *46*, 1830–1832.